Biomedical Optics EXPRESS

Multi-channel fiber photometry for population neuronal activity recording

Qingchun Guo,[1,2,6] Jingfeng Zhou,[3,4,6] Qiru Feng,[4] Rui Lin,[4] Hui Gong,[1,2] Qingming Luo,[1,2] Shaoqun Zeng,[1,2] Minmin Luo,[4,5,7] Ling Fu[1,2,*]

[1]*Britton Chance Center for Biomedical Photonics, Wuhan National Laboratory for Optoelectronics-Huazhong University of Science and Technology, Wuhan 430074, China*

[2]*MoE Key Laboratory for Biomedical Photonics, Department of Biomedical Engineering, Huazhong University of Science and Technology, Wuhan 430074, China*

[3]*PTN Graduate Program, School of Life Sciences, Peking University, Beijing 100081, China*

[4]*National Institute of Biological Sciences, Beijing 102206, China*

[5]*School of Life Sciences, Tsinghua University, Beijing 100084, China*

[6]*These authors contributed equally to this work*

[7]*luominmin@nibs.ac.cn*

[*]*lfu@mail.hust.edu.cn*

Abstract: Fiber photometry has become increasingly popular among neuroscientists as a convenient tool for the recording of genetically defined neuronal population in behaving animals. Here, we report the development of the multi-channel fiber photometry system to simultaneously monitor neural activities in several brain areas of an animal or in different animals. In this system, a galvano-mirror modulates and cyclically couples the excitation light to individual multimode optical fiber bundles. A single photodetector collects excited light and the configuration of fiber bundle assembly and the scanner determines the total channel number. We demonstrated that the system exhibited negligible crosstalk between channels and optical signals could be sampled simultaneously with a sample rate of at least 100 Hz for each channel, which is sufficient for recording calcium signals. Using this system, we successfully recorded GCaMP6 fluorescent signals from the bilateral barrel cortices of a head-restrained mouse in a dual-channel mode, and the orbitofrontal cortices of multiple freely moving mice in a triple-channel mode. The multi-channel fiber photometry system would be a valuable tool for simultaneous recordings of population activities in different brain areas of a given animal and different interacting individuals.

OCIS codes: (170.0170) Medical optics and biotechnology; (180.2520) Fluorescence microscopy; (170.2150) Endoscopic imaging; (170.2655) Functional monitoring and imaging.

References and links

1. M. J. Zigmond and F. E. Bloom, Fundamental neuroscience (Academic Press, 1999).
2. D. R. Humphrey and E. M. Schmidt, "Extracellular single-unit recording methods," in Neurophysiological techniques (Springer, 1990), pp. 1–64.
3. P. Anikeeva, A. S. Andalman, I. Witten, M. Warden, I. Goshen, L. Grosenick, L. A. Gunaydin, L. M. Frank, and K. Deisseroth, "Optetrode: a multichannel readout for optogenetic control in freely moving mice," Nat. Neurosci. **15**(1), 163–170 (2011).
4. J. Y. Cohen, S. Haesler, L. Vong, B. B. Lowell, and N. Uchida, "Neuron-type-specific signals for reward and punishment in the ventral tegmental area," Nature **482**(7383), 85–88 (2012).
5. Z. Liu, J. Zhou, Y. Li, F. Hu, Y. Lu, M. Ma, Q. Feng, J. E. Zhang, D. Wang, J. Zeng, J. Bao, J. Y. Kim, Z. F. Chen, S. El Mestikawy, and M. Luo, "Dorsal raphe neurons signal reward through 5-HT and glutamate," Neuron **81**(6), 1360–1374 (2014).
6. C. Stosiek, O. Garaschuk, K. Holthoff, and A. Konnerth, "In vivo two-photon calcium imaging of neuronal networks," Proc. Natl. Acad. Sci. U.S.A. **100**(12), 7319–7324 (2003).
7. T. Komiyama, T. R. Sato, D. H. O'Connor, Y. X. Zhang, D. Huber, B. M. Hooks, M. Gabitto, and K. Svoboda, "Learning-related fine-scale specificity imaged in motor cortex circuits of behaving mice," Nature **464**(7292), 1182–1186 (2010).

#246854 Received 27 Jul 2015; revised 31 Aug 2015; accepted 7 Sep 2015; published 10 Sep 2015

8. K. K. Ghosh, L. D. Burns, E. D. Cocker, A. Nimmerjahn, Y. Ziv, A. E. Gamal, and M. J. Schnitzer, "Miniaturized integration of a fluorescence microscope," Nat. Methods **8**(10), 871–878 (2011).
9. Y. Ziv, L. D. Burns, E. D. Cocker, E. O. Hamel, K. K. Ghosh, L. J. Kitch, A. El Gamal, and M. J. Schnitzer, "Long-term dynamics of CA1 hippocampal place codes," Nat. Neurosci. **16**(3), 264–266 (2013).
10. H. Adelsberger, O. Garaschuk, and A. Konnerth, "Cortical calcium waves in resting newborn mice," Nat. Neurosci. **8**(8), 988–990 (2005).
11. H. Lütcke, M. Murayama, T. Hahn, D. J. Margolis, S. Astori, S. M. Zum Alten Borgloh, W. Göbel, Y. Yang, W. Tang, S. Kügler, R. Sprengel, T. Nagai, A. Miyawaki, M. E. Larkum, F. Helmchen, and M. T. Hasan, "Optical recording of neuronal activity with a genetically-encoded calcium indicator in anesthetized and freely moving mice," Front. Neural Circuits **4**, 9 (2010).
12. C. Grienberger, H. Adelsberger, A. Stroh, R. I. Milos, O. Garaschuk, A. Schierloh, I. Nelken, and A. Konnerth, "Sound-evoked network calcium transients in mouse auditory cortex in vivo," J. Physiol. **590**(4), 899–918 (2012).
13. G. Cui, S. B. Jun, X. Jin, M. D. Pham, S. S. Vogel, D. M. Lovinger, and R. M. Costa, "Concurrent activation of striatal direct and indirect pathways during action initiation," Nature **494**(7436), 238–242 (2013).
14. A. Stroh, H. Adelsberger, A. Groh, C. Rühlmann, S. Fischer, A. Schierloh, K. Deisseroth, and A. Konnerth, "Making waves: initiation and propagation of corticothalamic Ca2+ waves in vivo," Neuron **77**(6), 1136–1150 (2013).
15. H. Adelsberger, C. Grienberger, A. Stroh, and A. Konnerth, "In vivo calcium recordings and channelrhodopsin-2 activation through an optical fiber," Cold Spring Harb Protoc 2014, pdb prot084145 (2014).
16. H. Adelsberger, A. Zainos, M. Alvarez, R. Romo, and A. Konnerth, "Local domains of motor cortical activity revealed by fiber-optic calcium recordings in behaving nonhuman primates," Proc. Natl. Acad. Sci. U.S.A. **111**(1), 463–468 (2014).
17. G. Cui, S. B. Jun, X. Jin, G. Luo, M. D. Pham, D. M. Lovinger, S. S. Vogel, and R. M. Costa, "Deep brain optical measurements of cell type-specific neural activity in behaving mice," Nat. Protoc. **9**(6), 1213–1228 (2014).
18. L. A. Gunaydin, L. Grosenick, J. C. Finkelstein, I. V. Kauvar, L. E. Fenno, A. Adhikari, S. Lammel, J. J. Mirzabekov, R. D. Airan, K. A. Zalocusky, K. M. Tye, P. Anikeeva, R. C. Malenka, and K. Deisseroth, "Natural neural projection dynamics underlying social behavior," Cell **157**(7), 1535–1551 (2014).
19. F. Fuhrmann, D. Justus, L. Sosulina, H. Kaneko, T. Beutel, D. Friedrichs, S. Schoch, M. K. Schwarz, M. Fuhrmann, and S. Remy, "Locomotion, theta oscillations, and the speed-correlated firing of hippocampal neurons are controlled by a medial septal glutamatergic circuit," Neuron **86**(5), 1253–1264 (2015).
20. Y. Chen, Y. C. Lin, T. W. Kuo, and Z. A. Knight, "Sensory detection of food rapidly modulates arcuate feeding circuits," Cell **160**(5), 829–841 (2015).
21. J. N. Betley, S. Xu, Z. F. Cao, R. Gong, C. J. Magnus, Y. Yu, and S. M. Sternson, "Neurons for hunger and thirst transmit a negative-valence teaching signal," Nature **521**(7551), 180–185 (2015).
22. T. W. Chen, T. J. Wardill, Y. Sun, S. R. Pulver, S. L. Renninger, A. Baohan, E. R. Schreiter, R. A. Kerr, M. B. Orger, V. Jayaraman, L. L. Looger, K. Svoboda, and D. S. Kim, "Ultrasensitive fluorescent proteins for imaging neuronal activity," Nature **499**(7458), 295–300 (2013).
23. M. A. Nicolelis, D. Dimitrov, J. M. Carmena, R. Crist, G. Lehew, J. D. Kralik, and S. P. Wise, "Chronic, multisite, multielectrode recordings in macaque monkeys," Proc. Natl. Acad. Sci. USA **100**(19), 11041–11046 (2003).
24. C. M. Lewis, C. A. Bosman, and P. Fries, "Recording of brain activity across spatial scales," Curr. Opin. Neurobiol. **32**, 68–77 (2015).
25. P. R. Roelfsema, A. K. Engel, P. König, and W. Singer, "Visuomotor integration is associated with zero time-lag synchronization among cortical areas," Nature **385**(6612), 157–161 (1997).
26. S. E. Morrison, A. Saez, B. Lau, and C. D. Salzman, "Different time courses for learning-related changes in amygdala and orbitofrontal cortex," Neuron **71**(6), 1127–1140 (2011).
27. M. Paukert, A. Agarwal, J. Cha, V. A. Doze, J. U. Kang, and D. E. Bergles, "Norepinephrine controls astroglial responsiveness to local circuit activity," Neuron **82**(6), 1263–1270 (2014).
28. M. Brecht, "Barrel cortex and whisker-mediated behaviors," Curr. Opin. Neurobiol. **17**(4), 408–416 (2007).
29. D. Feldmeyer, M. Brecht, F. Helmchen, C. C. Petersen, J. F. Poulet, J. F. Staiger, H. J. Luhmann, and C. Schwarz, "Barrel cortex function," Prog. Neurobiol. **103**, 3–27 (2013).
30. C. Zhan and M. Luo, "Diverse patterns of odor representation by neurons in the anterior piriform cortex of awake mice," J. Neurosci. **30**(49), 16662–16672 (2010).
31. A. Bechara, H. Damasio, and A. R. Damasio, "Emotion, decision making and the orbitofrontal cortex," Cereb. Cortex **10**(3), 295–307 (2000).
32. E. T. Rolls, "The orbitofrontal cortex and reward," Cereb. Cortex **10**(3), 284–294 (2000).
33. J. O'Doherty, M. L. Kringelbach, E. T. Rolls, J. Hornak, and C. Andrews, "Abstract reward and punishment representations in the human orbitofrontal cortex," Nat. Neurosci. **4**(1), 95–102 (2001).
34. T. A. Stalnaker, N. K. Cooch, and G. Schoenbaum, "What the orbitofrontal cortex does not do," Nat. Neurosci. **18**(5), 620–627 (2015).
35. J. Cha and J. U. Kang, "Spatially Multiplexed Fiber-optic Microscopy for Simultaneous Imaging of Multiple Brain Regions," in CLEO: Applications and Technology, (Optical Society of America, 2014), AF1B. 3.
36. J. Cha, D. Kim, G. W. Cheon, and J. U. Kang, "Spatially Multiplexed Fiber-optic SLM Microscopy for Applications of Optogenetics," in Imaging Systems and Applications, (Optical Society of America, 2015), IM4A. 2.
37. F. Helmchen and W. Denk, "Deep tissue two-photon microscopy," Nat. Methods **2**(12), 932–940 (2005).

#246854 Received 27 Jul 2015; revised 31 Aug 2015; accepted 7 Sep 2015; published 10 Sep 2015

38. S. P. Peron, J. Freeman, V. Iyer, C. Guo, and K. Svoboda, "A Cellular Resolution Map of Barrel Cortex Activity during Tactile Behavior," Neuron **86**(3), 783–799 (2015).
39. R. Frostig, *In Vivo Optical Imaging of Brain Function* (CRC press, 2002).

1. Introduction

Correlating neuronal responses with animal behavior plays a central role in the functional dissection of neural circuits in systems and behavioral neuroscience [1]. Traditional electrophysiology has the highest level of temporal accuracy, but falls short in the total recorded cell number and cell-type specificity [2]. By taking advantage of optogenetics, electrophysiology with "optical tagging" provides cell-type information for recorded cells [3–5]. However, this approach is technically challenging and often limited by low tagging efficiency. Two-photon microscopy could image a large volume of neurons in the cell-type specific manner, but is restricted to only superficial layers of cortical areas [6, 7] in anesthetized or head-restrained mice. Micro-optics using gradient refractive index (GRIN) lenses achieved fluorescence imaging from deep cells, although such imaging setups tend to be expensive and difficult [8, 9]. In addition, the large size of GRIN lens (>500 μm) indicates substantial invasiveness to brain tissues.

As an alternative, fiber photometry provides the most sensitive and easiest way to record cell-type specific population neuronal activities of the deep brain structures in behaving animals [10–20]. It employs one multimode optical fiber implanted in the brain. The excitation light is coupled into the multimode optical fiber, and the fluorescent signals of neuronal activity indicators return through the same optical fiber and are detected by a detector. Neurons of a given neurochemical phenotype in a defined brain structure often act collectively and synchronously to external or internal stimuli [4, 18, 21], thus manifesting large change in calcium signals as a functional ensemble. The genetically encoded calcium indicators (GECIs), such as GCaMP proteins [22], enable the photometry method to record the activity of genetically defined neuronal subclasses. Using fiber photometry, several groups have made exciting observations of neuronal activation patterns in the sensory and motor cortices [10–12, 14–16], basal ganglia [13], dopamine reward system [18], feeding circuits [20], basal forebrain [19], and have proposed new theories in each of these research fields.

In many cases, the multi-channel fiber photometry is valuable and even necessary for functional studies of neural circuits. Since neurons in different brain areas respond in coordination during specific task execution [23–26], activities in more than one brain areas need to be simultaneously recorded for investigating how signals in connected brain regions are integrated to produce behaviors. In addition, it is valuable and efficient to record from different animals that interact, such as during sociosexual behaviors, to study the neural correlates of social interaction. Efforts have already been made to develop dual-channel photometry devices. Adelsberger et al. recorded neural activities in two motor cortical regions simultaneously by using a two-sensor photometry device and showed that distinct subdomains of the motor cortex control specific movements [16]. Their paralleled dual-channel system adapted from the single-channel system by adding a new photon detector. However, this straightforward strategy would become inflexible and non-economical when more channels are needed, because a further increase in the channel number will change the basic structure of the system, requiring additional detectors and other optical elements and hence, more space. Paukert et al [27] recorded calcium transients of astrocytes in multiple brain areas by using a CCD camera through a fiber bundle, and demonstrated concurrent activation of astrocyte networks within the mouse brain. The channel number can be easily expanded in this system, but the use of CCD cameras limits the sensitivity and speed.

Here, we developed a new strategy for reliable and easily expandable multi-channel optical recording. We used a galvano-mirror to couple the excitation light cyclically to individual optical fibers of a custom-designed multimode fiber bundle. Multiple-site calcium signals can be acquired simultaneously through one detector at high sampling rates. The total channel number can be manipulated by fiber bundle assembly and scanner reconfiguration. Crosstalk between channels during data acquisition was extremely small, so that each fiber

#246854 Received 27 Jul 2015; revised 31 Aug 2015; accepted 7 Sep 2015; published 10 Sep 2015

channel sampled calcium signals simultaneously and independently. Testing in head-restrained and freely moving mice demonstrated that the system is highly sensitive, reliable, flexible, and simple to use.

2. Materials and methods

2.1 Optical setup

The basic structure of the multi-channel fiber photometry system was similar to the single-channel fiber recording system that has been reported by several groups [15, 17, 18]. As shown in Fig. 1(A), 488 nm excitation light from a semiconductor laser (Coherent, Inc. OBIS 488 LS, tunable power up to 60 mW) was reflected by a dichroic mirror with a 452–490 nm reflection band and a 505–800 nm transmission band (Thorlabs, Inc. MD498), and then coupled to a multimode fiber (Thorlabs, Inc., 200 μm in diameter and 0.39 in numerical aperture) by an objective (JiangNan, Inc. 20 × , NA 0.4). The emission fluorescence was collected with the same optical fiber and then detected by a high sensitive photomultiplier tube (PMT) (Hamamatsu, Inc. H10720-210) after filtering by a GFP bandpass emission filter (Thorlabs, Inc. MF525-39). To increase the channel number, we replaced the single optical fiber with a custom-designed multimode optical fiber bundle (Fig. 1(B)). In addition, a galvano mirror (Thorlabs, Inc. GVS001) was placed between the laser and the dichroic mirror. Through the scanning of the galvano mirror, the excitation light was coupled to each fiber in the optical fiber bundle. The sample rate for each channel was set to 100 Hz since the kinetics of calcium signal is relatively slow [10, 22]. This procedure thus resembled time division multiplexing (TDM) in communication. Furthermore, the channel number could be easily changed by assembling the fiber bundles and reconfiguring the scanner control voltage, without the necessity to change the system structure as in the conventional multi-channel system [16].

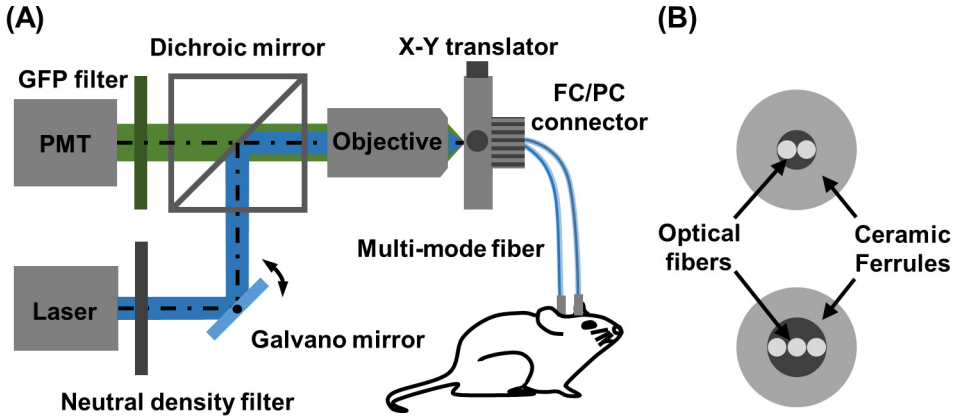

Fig. 1. Multi-channel fiber photometry system. (A) Schematic diagram of the extensible multi-channel fiber photometry system. A 488 nm laser is successively coupled to each multimode optical fiber by using the galvano mirror. The excited fluorescent light is then collected by the same optical fiber and detected by the PMT. (B) Schematic diagram of the custom designed multimode fiber bundles for the dual-channel mode (upper) and the triple-channel mode (lower). Both types of fiber bundles are custom designed. Each comprises of the corresponding number of multimode optical fibers aligned in the form of a single line and fixed into the ceramic ferrules.

2.2 Data acquisition and preprocessing

This multi-channel system contained only one photon detector, which streamed analog data into a DAQ card (National Instruments Inc. USB-6001). Therefore, the signals collected from

#246854 Received 27 Jul 2015; revised 31 Aug 2015; accepted 7 Sep 2015; published 10 Sep 2015

different channels were multiplexed and hence, needed to be separated before further data display and analysis. We implemented an online data-demultiplexing algorithm to reorganize the raw data into different channels (Fig. 2). Briefly, the sampled raw data was grouped into different channels based on the coupling frequency, which was determined by the control voltage of the galvano mirror. The grouped data was then averaged to reduce high frequency noise and was separated into different channels. The separated signals were filtered by a low-pass filter (cut-off frequency = 30 Hz) before displaying and saving in the computer.

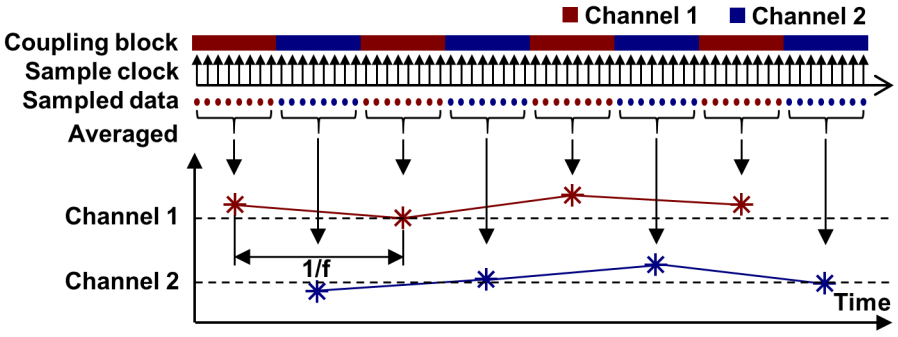

Fig. 2. Schematic representation of data acquisition and channel separation for the 2-channel system. The coupling blocks are used to represent the time when the laser is coupled to one of the fibers. Red color is for channel 1 while blue is for channel 2. During recording, the sample clock rate of the DAQ card is several times larger than the sample frequency (f = 100 Hz). The sampled data was grouped according to the coupling block and then averaged to an actual sample value for each channel.

2.3 Animals

The BAC-transgenic mouse strain CaMKIIα-Cre were acquired from the Jackson Laboratory [B6.Cg-Tg(Camk2a-cre)T29-1Stl/J]. They were backcrossed and maintained in a C57BL/6J background and housed in groups on a reverse 12 hr light/dark cycle with food and water *ad libitum*. Adult mice of either sex (8-16 weeks old) were water-deprived 36 hours before behavioral tests and optical recording. All procedures were conducted with the approval of the Institutional Animal Care and Use Committee (IACUC) of the National Institute of Biological Sciences (NIBS), Beijing, China.

2.4 Viral vector preparation

We used the Cre-dependent adeno-associated virus (AAV) with double-floxed inverted open reading frames (DIO) of the GCaMP6m coding sequence in the inverted direction (AAV-EF1a-DIO-GCaMP6m). The GCaMP6m sequence was cloned from the pGP-CMV-GCaMP6m plasmid (a gift from Douglas Kim, Addgene plasmid #40754) [19]. The pAAV-EF1a-EGFP-IRES-WGA-Cre vector was engineered from pAAV-EF1a-mCherry-IRES-WGA-Cre (a gift from Karl Deisseroth) by replacing the mCherry with the EGFP. Both vectors were packaged into AAV vectors of serotype 2/9, which consist of AAV2 ITR genomes pseudotyped with AAV9 serotype capsid proteins. The final titers of these two viral vectors were between 1 and 10×10^9 particles/μL.

2.5 Animal surgery and virus injection

Before viral injection, the mouse was anesthetized with pentobarbital (i.p., 80 mg/kg) and head restrained in a stereotaxic instrument. After disinfection with 0.3% hydrogen peroxide, a small skull area above the targeted cortical area was exposed. For viral injection of barrel cortices, two small 1-mm diameter holes in the skull were drilled (AP: −1.4 mm, ML: ± 3 mm, DV: 0.4 mm) and 300 nL AAV-DIO-GCaMP6m virus was pressure injected into

#246854 Received 27 Jul 2015; revised 31 Aug 2015; accepted 7 Sep 2015; published 10 Sep 2015

bilateral barrel cortices or one side of orbitofrontal cortex through a pulled glass pipette (Sutter Instrument) at a speed of 40 nL/min using a Nanoliter 2000 (WPI). The glass pipette was withdrawn 10 min later. Optical fibers that were held within a ceramic ferrule were implanted at the same site. For the recording of the orbitofrontal cortex, 300 nL mixture of AAV-DIO-GCaMP6m and AAV-Cre virus (3:1) were injected into the C57BL/6J mice (AP: 2.5 mm, ML: 1.5 mm, DV: 1.5 mm). The mice were then placed in their home cage for recovery and viral transgene expression.

2.6 Histology and imaging

After fiber optics recording, mice were sacrificed with overdose injection of pentobarbital (i.p., 300 mg/kg) and then intracardially perfused with 0.9% saline solution followed by 4% paraformaldehyde (PFA) in PBS. Mouse brains were kept in 4% PFA solution overnight for post fixation and then cryoprotected in 30% sucrose solution for 2 days. Coronal sections (50 μm thick) around the fiber implanting sites were prepared with a freezing cryostat (Leica CM1900). Brain sections were mounted on chrome-gelatin subbed glass slides and cover slipped with 50% glycerol mounting medium. Fluorescent images were acquired with an auto imaging system (EVOSTM FL Auto Imaging System) using 4 × and 10 × objectives for the orbitofrontal cortex and barrel cortex, respectively. Global brightness and contrast of these images were adjusted to reduce background and green pseudocolor was added to represent the GFP fluorescence.

3. Results

3.1 Scanner control and system characterization in the dual-channel mode

In the dual-channel mode, the ceramic ferrule contained two multimode optical fibers, each of which directed guided light for the two separate channels (Fig. 3(A)). For illustration purpose in Fig. 3, we use the color red or blue to distinguish the two channels (red for channel 1 and blue for channel 2). The voltage-controlled galvano mirror deflected light at angles based on input voltages. Three voltage levels (U, 0, -U) were used to configure the two channels (Fig. 3(A)). The excitation light was cyclically coupled to the channel 1 fiber at the voltage level of U and to channel 2 fiber at the voltage level of –U. For scanner protection, level 0 was set as an intermediate state with a constant duration of 0.83 ms in each cycle, so that the angle of scanner won't change straightly between channel 1 and channel 2.

#246854 Received 27 Jul 2015; revised 31 Aug 2015; accepted 7 Sep 2015; published 10 Sep 2015

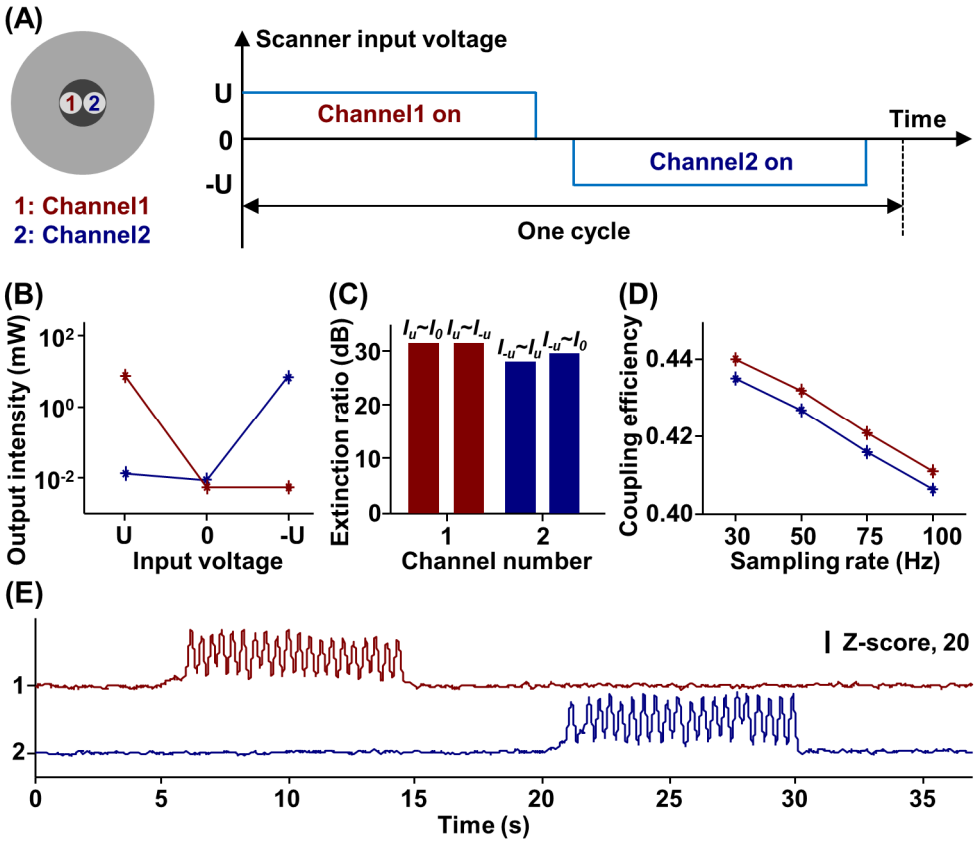

Fig. 3. The scanner control method and system performance evaluation in the dual-channel mode. (A) Scanner control waveform for dual-channel mode. Red and blue colors are used to represent channel 1 and channel 2, respectively. The scanner input voltage was set to U for channel 1 detection and –U for channel 2 detection. It was set to 0 for scanner protection. The time of one cycle equals the multiplicative inverse of the sampling frequency. (B) The output intensity at the distal end of two individual optical fibers when the scanner input voltage was set to U, 0, and –U. (C) The extinction ratio of each channel. (D) The coupling efficiency of each channel with varying sampling rates. (E) Autofluorescence signals acquired in the dual-channel mode with a white paper as sample.

In a multi-channel system, crosstalk between different channels should be avoided. We measured the output intensity of the two channels during the light-coupled ("on") state and uncoupled ("off") states to evaluate the potential crosstalk between channels. For both channels, the output intensities of light-coupled state were several orders of magnitude greater than that of the uncoupled state (Fig. 3(B)). Furthermore, we calculated the extinction ratio of each channel by the equation:

$$Ext = 10\log_{10}(I_{on} / I_{off}), \tag{1}$$

where I_{on} and I_{off} are the output intensities of the fiber in the "on" and "off" state, respectively; the unit of the extinction ratio is dB. For channel 1, the output intensity in "on" state is I_u, while the output intensity in "off" state are I_0 and I_{-u}. The extinction ratios of both channels were above 25 dB (Fig. 3(C)), indicating the crosstalk in our system was negligible.

Figure 3(D) shows the coupling efficiency of both channels at various sampling rates. In the scanning mode, the light was coupled to the measured fiber only during its "on" state, so that the averaged output intensity was discounted compared with a continuous coupling mode, and the measured coupling efficiency was blow 50%. Because the duration of the "0" state

#246854 Received 27 Jul 2015; revised 31 Aug 2015; accepted 7 Sep 2015; published 10 Sep 2015

remained constant in each cycle, the coupling efficiency decreased slightly (~3%) when the sampling rate increased from 30 Hz to 100 Hz. However, the discretely sampled fluorescent signal from each channel was not influenced by this scanning mode.

We further tested the dual-channel mode by acquiring autofluorescence signals from a white paper (Fig. 3(E)). By successively moving the white paper back and forth, we observed the intensity fluctuation and calculated the Z-score of the signals using the following equation:

$$Z = (F - F_0) / \sigma F, \tag{2}$$

where F is the test signal, F_0 and σF are the mean and standard deviation of the basal signal, respectively. The intensity fluctuation appears only in the tested channel, demonstrating that signals from one channel did not cross into the other channel.

3.2 Scanner control and system characterization in the triple-channel mode

In the triple-channel mode, the fiber bundle consisted of three multimode optical fibers that were aligned into a horizontal line (Fig. 4(A)). Three voltage levels (U, 0, -U) were used for coupling the excitation light into each optical fiber: U for channel 1, 0 for channel 2 and -U for channel 3 (Fig. 4(A)).

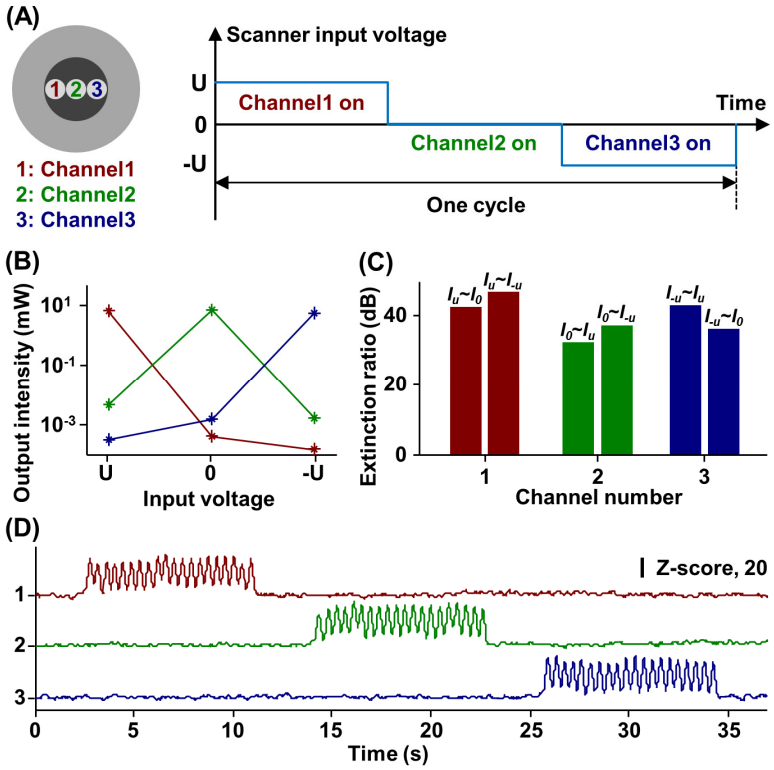

Fig. 4. Scanner control and system performance of triple-channel mode. (A) Scanner control waveform for the triple-channel mode. Red, green, and blue colors represent channel 1, 2, and 3, respectively. The scanner input voltage was set to U for channel 1 detection, 0 for channel 2, and –U for channel 3. The time of one cycle equals the multiplicative inverse of the sampling frequency. (B) The output intensity at the distal end of each optical fiber in three states of the scanner. (C) The extinction ratio of each channel. (D) Autofluorescence signals acquired in the triple-channel mode with a white paper as sample.

#246854 Received 27 Jul 2015; revised 31 Aug 2015; accepted 7 Sep 2015; published 10 Sep 2015

We similarly evaluated the potential crosstalk between channels. Figure 4(B) shows the output intensity at the distal end of each optical fiber in three states of the galvano-mirror, while Fig. 4(C) shows the extinction ratio. The difference in the output intensities of "on" and "off" states was ~4 orders of magnitude for each channel. The extinction ratio was above 30 dB in all cases. We further tested the isolation performance of the triple-channel mode with a white paper (Fig. 4(D)). We observed fast fluctuations with a high signal-to-noise ratio only in the tested channel. Thus, the influence of channel crosstalk is also negligible in the triple-channel fiber photometry system.

3.3 Simultaneous recording of calcium signals from the bilateral barrel cortices of a head-restrained mouse

We tested the performance of the dual-channel fiber photometry system by recording calcium signals from the bilateral barrel cortices of behaving mice. The neural activity of rodent barrel cortex is correlated with the whisker movement in the opposite side of the body [28, 29]. By using the dual-channel mode of our system, population activities of bilateral barrel cortices were recorded simultaneously. CaMKIIα-Cre mice were injected with AAV-DIO-GCaMP6m viral vectors into the barrel cortex of both hemispheres (Fig. 5(A)). Two optical fibers were implanted at the sites of virus injection. After two weeks, GCaMP6 protein was expressed in the primary somatosensory cortex barrel field (abbreviated as S1BF) (Fig. 5(B)).

#246854 Received 27 Jul 2015; revised 31 Aug 2015; accepted 7 Sep 2015; published 10 Sep 2015

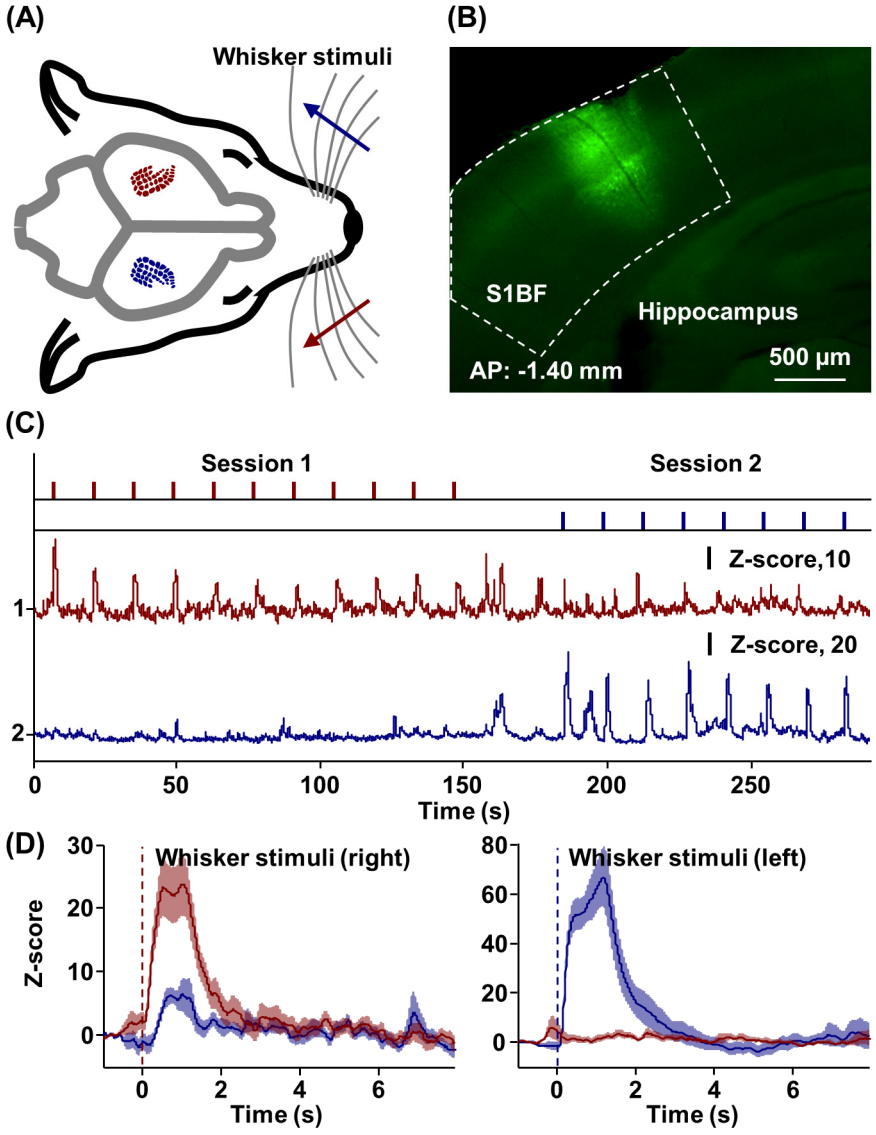

Fig. 5. Simultaneous recording of calcium signal from the bilateral barrel cortices in a head-restrained behaving mouse. (A) Schematic diagram of the whisker stimulation experiment. Channels 1 and 2 detected the left and right barrel cortex, respectively. We stimulated whiskers using a trigger-controlled air stream. The trigger signal and the calcium signal were synchronously recorded. (B) GCaMP6 expression (green) in the barrel cortex. The coronal slice is 1.4 mm posterior to bregma. Abbreviations: S1BF, primary somatosensory cortex, barrel field. (C) Calcium signals acquired simultaneously in the bilateral barrel cortices during the whisker stimulation experiment. The red and blue vertical bars mark the time given for the right and left whisker stimulation, respectively. (D) Averaged calcium transient in response to the contralateral whisker stimulation. Red and blue indicate signals from channel 1 and 2. Solid lines represent average calcium transients, whereas the shaded areas indicate SEM.

We recorded calcium transients from a head-restrained behaving mouse on an air-floating spherical treadmill [30]. After the mouse became habituated by walking on the treadmill for 30 minutes, two optical fibers from the dual-channel fiber bundle were individually connected to the brain-implanted optical fibers through ceramic ferrules. We stimulated the whiskers of either side by applying airstream. Stimulating the whiskers of one side evoked strong calcium transients in the contralateral but not ipsilateral barrel cortex (Fig. 5(C)). The responses to

#246854 Received 27 Jul 2015; revised 31 Aug 2015; accepted 7 Sep 2015; published 10 Sep 2015

repeated stimulations gradually decreased, suggesting response adaptation of the barrel cortex to whisker stimulation. After the experiments, we aligned and analyzed the calcium signals across 11 or 8 trials for the two stimulation blocks (Fig. 5(D)) and confirmed that whisker stimulation of one side produced strong and significant neural responses in the barrel cortex of the opposite hemisphere. Thus, two brain areas within the same animal could be simultaneously recorded using the dual-channel fiber photometry system.

3.4 Simultaneous recording from the orbitofrontal cortices of freely moving mice

We tested the performance of the triple-channel fiber photometry system by simultaneously recording calcium signals from the orbitofrontal cortex (OFC) of three individual behaving mice. The orbitofrontal cortex (OFC) is an important brain region for sensory integration, reward processing, emotion regulation, and decision-making [31–34]. We examined whether the system could detect reward-associated neuronal activation by allowing thirsty mice to lick for sucrose solution (Fig. 6(A)). GCaMP6m was expressed in the OFC of C57BJ/6 mice by injecting a mixture of AAV-Cre and AAV-DIO-GCaMP6m viral vectors. One optical fiber was implanted after each mouse was injected by the virus. We observed GCaMP6 expression exclusively in the OFCs after two weeks (Fig. 6(B)).

After water-deprivation for 36 hours, three mice that were implanted with a recording fiber were individually placed in separate cages. A small bottle of sucrose solution was placed in each cage and retrieved 5 seconds after sucrose lick. The GCaMP signals of OFC neurons increased and continued to ramp up when a mouse approached the sucrose solution. In addition, the activities started to drop following sucrose consumption (Fig. 6(C)). We also found spontaneous calcium fluctuations between sessions, possibly indicating reward seeking behaviors. However, we did not observe any concurrent responses in neural activities between the three animals, which could not be attributed to chance. Again, the aligned and averaged neuronal responses clearly demonstrate that there was no crosstalk between the calcium signals recorded from the three animals (Fig. 6(D)).

#246854 Received 27 Jul 2015; revised 31 Aug 2015; accepted 7 Sep 2015; published 10 Sep 2015

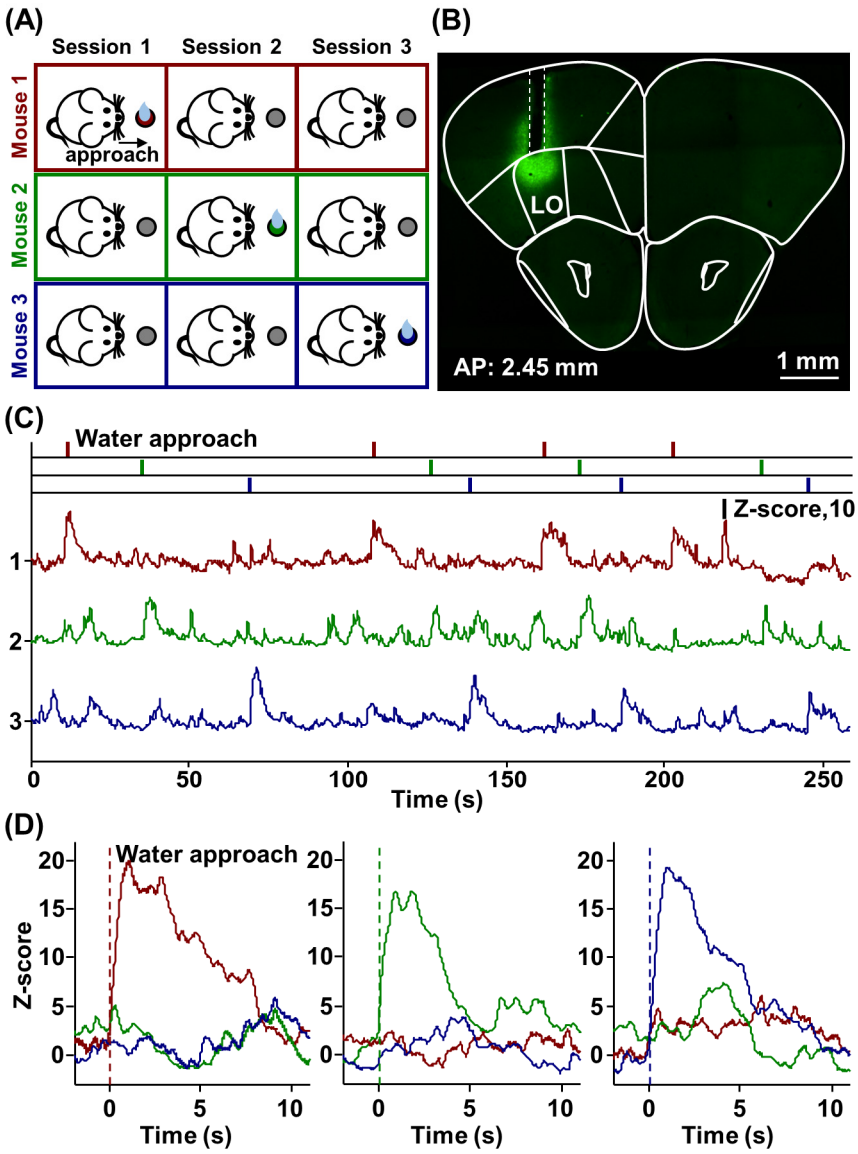

Fig. 6. Simultaneous recording of calcium signal from the orbitofrontal cortices (OFC) of three freely moving mice. (A) Schematic diagram of the water approach experiment. Each channel was used to record from the OFC of one thirsty mouse. Only one mouse was allowed to approach sucrose solution at any given moment, (B) Fluorescent photomicrograph of a coronal slice showing GCaMP6m expression in the OFC. The coronal slice is 2.45 mm anterior to bregma. The dashed line shows where the fiber has been implanted. Abbreviations: LO, lateral orbital cortex. (C) Calcium signals acquired simultaneously in the three freely moving mice during the water approach experiment. The red, green, and blue vertical bars mark the time at which the corresponding mouse approached the water. (D) Averaged calcium transient from the three individual mice. Red, green, and blue solid lines represent signals from channels 1, 2, and 3, respectively. Signals were aligned by water approach by mouse 1, 2, and 3 for the left, middle, and right panels, respectively.

4. Conclusion and discussion

We developed an easily expandable multi-channel fiber photometry system for recording calcium signals from freely moving mice. We improved the design of the conventional single-

#246854 Received 27 Jul 2015; revised 31 Aug 2015; accepted 7 Sep 2015; published 10 Sep 2015

channel optical fiber photometry by adding a galvano mirror and replacing the single multimode fiber with a custom-designed multimode optical fiber bundle. The galvano mirror modulates the excitation light and then couples it into each optical fiber with a cycling frequency equal to the sampling rate. Calcium signals from multiple brain regions can be simultaneously acquired at a high sample rate (100 Hz per channel). Channel number of this system can be increased by adjusting the fiber bundle topology and the scanner control program, without modification of the basic structure of the system. Our system exhibits a high performance, especially of the minimal crosstalk between channels. *In vivo* recordings in the barrel cortex and the OFC demonstrate that this system is both sensitive and stable for recording from freely-moving animals.

Our design has the advantages of simplicity and further expandability. The previous design of dual-channel photometry requires separate photo detector for each channel and additional light splitting and light coupling devices [16]. The system using the CCD camera [27] falls short in sensitivity and speed. In contrast, we can change our system to any reasonable number of channels using custom-designed fiber bundles with different number of optical fibers, without changing the basic composition of the system. The maximal channel number that can be obtained in this system is only restricted by the sweeping range of the scanner. Moreover, by adding another scanner, optical fibers can be arranged in a two dimensional topology, such that the maximal channel number can be quadratically increased. Because of the high quantum efficiency of PMT, the sensitivity of this system should remain high even when the channel numbers is further increased. In addition, laser scanning may be applied for simultaneous calcium imaging [35] and optogenetic stimulation [36] of multiple brain regions using fiber bundles.

The development of calcium fluorescent probes, especially the genetically encoded calcium indicators (GECIs) has promoted the optical imaging and recording methods of measuring calcium levels as the proxies of cell-type specific neuronal activities [13, 18–20]. Compared to electrophysiology and other sophisticated imaging methods [6, 37–39], the fiber photometry is easy, convenient, and stable for *in vivo* monitoring of population neuronal activities, especially in the deep brain regions such as the striatum, amygdala and hypothalamus. Our system is not only suitable for recording neural activities of different brain regions of the same animal, but is also suitable for recordings in different animals. Therefore, the multi-channel fiber photometry could be applied to study the neural circuit mechanisms underlying various animal behaviors.

Acknowledgments

This work was supported by Science Fund for Creative Research Group of China (61421064), National Natural Science Foundation of China (61178077&91432114), China MOST grants (2012CB837701 & 2012YQ03026005), and Beijing Municipal Government.

#246854 Received 27 Jul 2015; revised 31 Aug 2015; accepted 7 Sep 2015; published 10 Sep 2015